The influence of implant diameter and length on stress distribution of osseointegrated implants related to crestal bone geometry: A three-dimensional finite element analysis

Luigi Baggi, DDS,[a] Ilaria Cappelloni, MS,[b] Michele Di Girolamo, DDS,[c] Franco Maceri, MS,[d] and Giuseppe Vairo, MS, PhD[e]
University of Rome "Tor Vergata," School of Dentistry and School of Medical Engineering, Rome, Italy

Statement of problem. Load transfer mechanisms and possible failure of osseointegrated implants are affected by implant shape, geometrical and mechanical properties of the site of placement, as well as crestal bone resorption. Suitable estimation of such effects allows for correct design of implant features.

Purpose. The purpose of this study was to analyze the influence of implant diameter and length on stress distribution and to analyze overload risk of clinically evidenced crestal bone loss at the implant neck in mandibular and maxillary molar periimplant regions.

Material and methods. Stress-based performances of 5 commercially available implants (2 ITI, 2 Nobel Biocare, and 1 Ankylos implant; diameters of 3.3 mm to 4.5 mm, bone-implant interface lengths of 7.5 mm to 12 mm) were analyzed by linearly elastic 3-dimensional finite element simulations, under a static load (lateral component: 100 N; vertical intrusive component: 250 N). Numerical models of maxillary and mandibular molar bone segments were generated from computed tomography images, and local stress measures were introduced to allow for the assessment of bone overload risk. Different crestal bone geometries were also modelled. Type II bone quality was approximated, and complete osseous integration was assumed.

Results. Maximum stress areas were numerically located at the implant neck, and possible overloading could occur in compression in compact bone (due to lateral components of the occlusal load) and in tension at the interface between cortical and trabecular bone (due to vertical intrusive loading components). Stress values and concentration areas decreased for cortical bone when implant diameter increased, whereas more effective stress distributions for cancellous bone were experienced with increasing implant length. For implants with comparable diameter and length, compressive stress values at cortical bone were reduced when low crestal bone loss was considered. Finally, dissimilar stress-based performances were exhibited for mandibular and maxillary placements, resulting in higher compressive stress in maxillary situations.

Conclusions. Implant designs, crestal bone geometry, and site of placement affect load transmission mechanisms. Due to the low crestal bone resorption documented by clinical evidence, the Ankylos implant based on the platform switching concept and subcrestal positioning demonstrated better stress-based performance and lower risk of bone overload than the other implant systems evaluated. (J Prosthet Dent 2008;100:422-431)

Clinical Implications

Numerical results suggest that implant diameter may be more effective than implant length as a design parameter to control the risk of bone overload. For a given implant in the molar region, the worst load transmission mechanisms arise with maxillary placement, and implant biomechanical behavior greatly improves if bone is efficiently preserved at the crest.

[a]Associate Professor, School of Dentistry.
[b]PhD student, School of Medical Engineering.
[c]Assistant Professor, School of Dentistry.
[d]Full Professor, School of Medical Engineering.
[e]Assistant Professor, School of Medical Engineering.

Endosseous dental implants are currently used to retain and/or support prostheses for restoring completely or partially edentulous patients, for a variety of tooth loss scenarios. Whether an implant is used following a period of undisturbed healing or immediately after placement, a number of clinical studies[1-11] have shown that failure of osseointegrated implants is generally not related to mechanical failure of the load-bearing artificial structure (generally titanium based), but is induced by bone weakening or loss at the periimplant region. Moreover, clinical research has documented that the incidence of implant failure in the maxillary posterior region is generally higher than in the mandibular posterior area.[7-11]

Bone resorption can be activated by surgical trauma or bacterial infection, as well as by overloading at the bone-implant interface.[2,12-15] Under functional forces, overloading of periimplant bone can be induced by a shortcoming in load transfer mechanisms, primarily due to improper occlusion, prosthesis and/or implant design, and surgical placement. As a consequence, high stress concentrations at the bone-implant interface may arise and, according to well-supported hypotheses,[14-17] related strain fields in bone tissue may stimulate biological bone resorption, jeopardizing implant effectiveness.

Bone resorption at the implant neck (usually called "cratering") is not inevitable, because some clinical evidence has indicated that a reduction of crestal bone loss is possible when the connection diameter of the abutment is narrower than the implant collar; that is, when so-called platform switching configurations are considered.[18-20] Combining this concept with subcrestal placement and a microstructured implant, bone apposition on the horizontal surface of the implant should be accomplished, transferring the biological width from the vertical to the horizontal level (platform shifting). Accordingly, although platform switching configurations can suffer higher stress gradients and stress values in the abutment or abutment screw, additional support for overlying soft tissues is provided, inducing a more complete implant integration[21-23] and ensuring excellent esthetics over the long term. The reasons that platform switching results in bone preservation have not yet been clarified, but several hypotheses are related to the location of the microgap between the implant and the abutment, as well as to stress distribution at periimplant regions.[24-27]

Stress and strain fields around osseointegrated dental implants are affected by a number of biomechanical factors, including the type of loading, material properties of the implant and the prosthesis, implant geometry, surface structure, quality and quantity of the surrounding bone, and the nature of the bone-implant interface.[12,13] As far as implant shape is concerned, design parameters that primarily affect load transfer characteristics (the stress/strain distributions in the bone) include implant diameter and the length of the bone-implant interface, as well as, in the case of threaded implants, thread pitch, shape, and depth. To increase the surface area for osseous integration, threaded implants are generally preferred to smooth cylindrical ones.[28] Depending on bone quality, surface treatments and a thread geometry can significantly influence implant effectiveness, in terms of both initial stability and the biomechanical nature of the bone-implant interface after the healing process.[29,30]

Several implant concepts have been developed, and many implant types are commercially available in different sizes, shapes, materials, and surfaces. To analyze the effectiveness and reliability of endosseous implants, revealing possible risks of implant failure, stress analysis of bone-implant mechanical interactions is important.[31,32]

The complex geometry of the coupled bone-implant biomechanical system prevents the use of closed-form approach for stress evaluation. Therefore, the behavior of endosteal dental implants can be investigated by using numerical techniques. Recently, the finite element method has been widely applied to prosthetic dentistry[33,34] to predict stress and strain distributions at periimplant regions, investigating the influences of implant and prosthesis designs,[35-43] the magnitude and direction of loads,[41-45] and bone mechanical properties,[46,47] as well as modelling different clinical scenarios.[20,48-52] Some authors consider axisymmetric or bidimensional simplified models,[39,41,42] disregarding the proper shape of the placement site and/or the implant, as well as the effects of clinically evidenced crestal bone loss in functioning implants, that is, after a healing and loading period.[53,54] Nevertheless, more realistic results can be obtained through a more detailed modelling of implant and bone (including possible crater-like bone resorption effects), as well as suitable boundary conditions that do not affect local stress distribution at the bone-implant interface.

The purpose of this study was to compare, by means of 3-dimensional (3-D) linearly elastic finite element simulations, load transmission mechanisms and bone overload risk of 5 commercial osseointegrated implants in functioning conditions, modelling clinically evidenced crestal bone geometry. Different implant-abutment connections were considered, including platform switching configurations. Moreover, with the purpose of investigating the influence of the site of placement, placement of implants in both maxillary and mandibular molar bone segments were numerically compared.

MATERIAL AND METHODS

Five threaded dental implants were analyzed (Fig. 1, A): 2 ITI Standard implants (Institut Straumann AG, Basel, Switzerland), 2 Nobel Biocare implant systems (Nobel Bio-

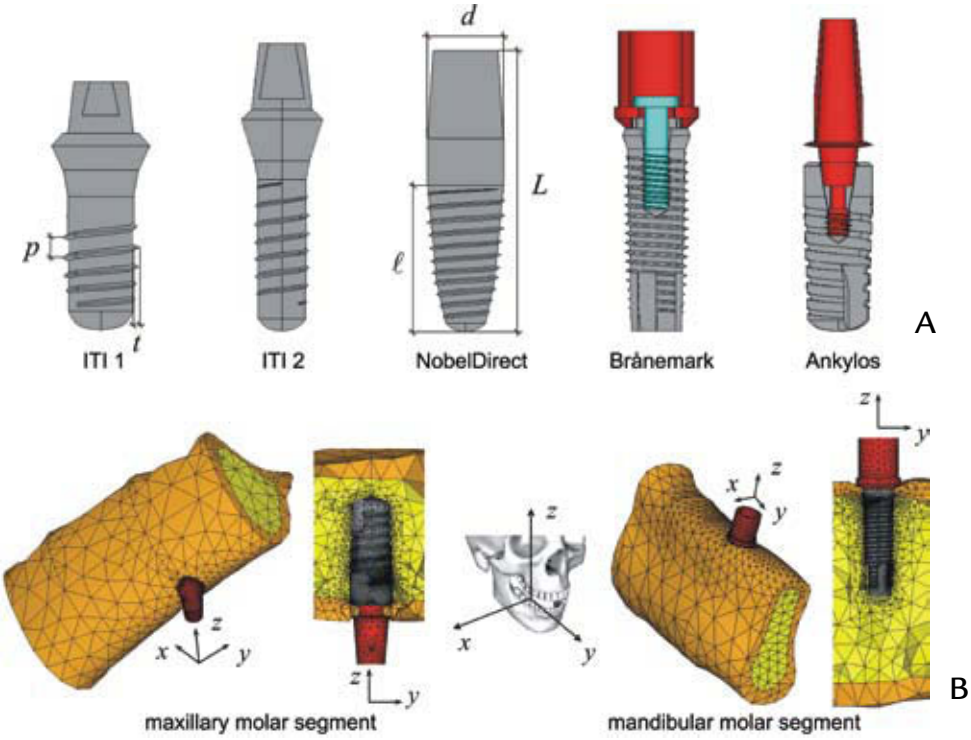

1 A, Solid models of 5 implant systems analyzed (*L*: implant total length; ℓ : bone-implant interface length; *d*: implant maximum diameter; *p*: average thread pitch; *t*: average thread depth). B, Mesh details of overall bone-implant system for both maxillary and mandibular bone segments.

TABLE I. Geometric properties of 5 implants analyzed in this study. Notation refers to Figure 1: *L* is implant total length; ℓ denotes bone-implant interface length; *d* indicates implant maximum diameter; *p* is average thread pitch; *t* is average thread depth

Implant	*L* (mm)	ℓ (mm)	*d* (mm)	*p* (mm)	*t* (mm)	Manufacturer
ITI Standard (1)	16	7.5	4.10	1.15	0.24	Institut Straumann AG,
ITI Standard (2)	17	9.0	3.30	0.98	0.20	Basel, Switzerland
NobelDirect	16	9.0	4.50	0.73	0.21	Nobel Biocare AB,
Brånemark System	14	12.0	3.75	0.60	0.27	Göteborg, Sweden
Ankylos	11	11.0	4.50	1.06	0.20	Dentsply Friadent, Mannheim, Germany

care AB, Göteborg, Sweden), and an Ankylos implant (Dentsply Friadent, Mannheim, Germany). The ITI and NobelDirect implants were modelled by a 1-body structure; the Brånemark implant is connected to the abutment by an internal screw; the Ankylos system has a threaded abutment directly inserted into the implant, and in agreement with the platform switching concept. The thread is trapezoidal for the Ankylos implant and triangular for the other implants. As summarized in Table I, implants are comparable in thread pitch and depth, whereas the diameter varies from 3.3 mm to 4.5 mm, and the length of the implant-bone interface varies from 7.5 mm to 12 mm.

Three-dimensional solid models of implants and abutments were developed by using a comparative technique involving high-resolution pictures and actual implants. Maxillary and mandibular bone segments relevant to molar regions were modelled from CT (computed tomography) images, evaluating the physiological parameters of cancellous and compact bone with software (SimPlant 7.0; Materialise Dental NV, Leuven, Belgium). Gingival soft tissues were not modelled, and bone segments were modelled with 2 volumes (Fig. 1, B): an outer shell with an average thickness of about 2 mm, representing the

cortical bone layer, and an inner volume representing cancellous bone tissue, assumed to be perfectly connected with the cortical layer. The length of bone segments in the mesial-distal direction (Fig. 1, *y* axis) was approximately 40 mm, and the average height was about 16 mm for the maxillary segment and 24 mm for the mandibular segment. Implant systems were assumed to be placed approximately at the midspan of bone segments.

To realistically reproduce the physiological structure of the compact bone arising around a functioning implant after a healing period, different periimplant crestal geometries were modelled. Depending on implant shape and in accordance with well-established clinical evidence (Fig. 2, A),[53,54] 2 types of crestal bone geometries were considered in detail. As shown in Figure 2, a "flared" shape was modelled for ITI and Nobel Biocare implants, accounting for a cratering effect with a mean crestal bone loss of about 45% in thickness. For the Ankylos implant, the platform switching configuration indicated low crestal bone loss (assumed to be about 20% in thickness) should be modeled with a horizontal cortical bone layer apposition of about 0.3 mm in thickness.

All 3-D solid models (bone segments and implants) were built using a custom-made preprocessing tool, developed as a part of a commercial software program (MATLAB; The MathWorks, Inc, Natick, Mass), which is able to produce the primary topology of each model through a cubic interpolation algorithm. Its output is fully compatible with a commercial finite element code (ANSYS 7.1; ANSYS, Inc, Canonsburg, Pa) used for merging all of the parts comprising the overall bone-implant model and for generating and solving the discrete finite element meshes.

Numerical models of implants in maxillary and mandibular bone segments were generated by means of 10-node tetrahedral elements based

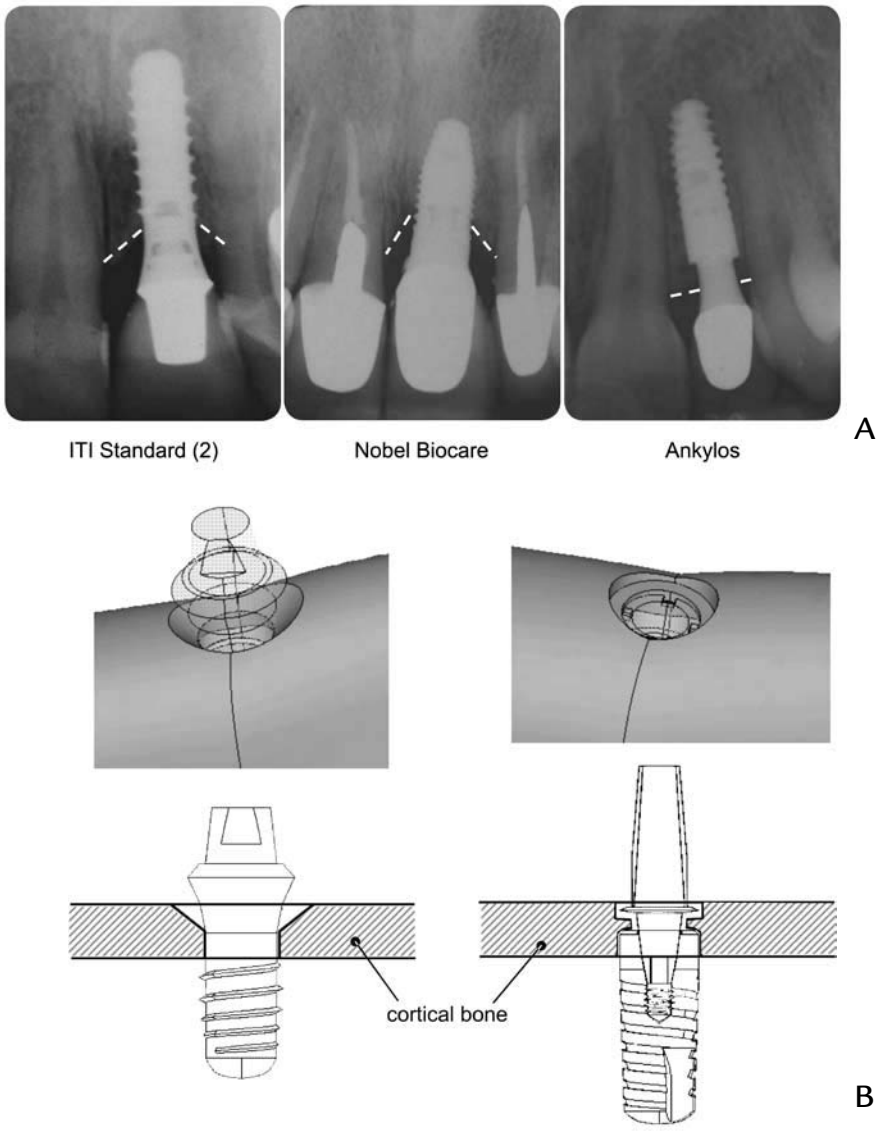

2 Geometrical modelling of crestal bone loss induced by implant shape. A, Periapical radiographs showing crestal bone loss for ITI Standard (2), Nobel Biocare, and Ankylos implants after loading period of approximately 1 year. B, Bone solid models relevant to situation of significant cratering crestal bone loss (left) and to situation of low bone loss, due to platform switching configuration and subcrestal placement (right).

on a pure displacement formulation, with quadratic displacement shape functions and 3 degrees of freedom per node.[55] Resulting from an optimization process based on numerical convergence analyses, mean value of the mesh size was set equal to approximately 0.6 mm for the bone-implant interface, and to approximately 0.1 mm at the periimplant region. Table II summarizes the number of elements and nodes for the convergent discrete models.

Dry material models were used for bone tissues, neglecting the effects of fluid-solid interactions. Materials were assumed to have a linearly elastic isotropic behavior, and all material volumes were considered to be homogeneous. Implants and abutments were assumed to be constituted of a titanium alloy, Ti6Al4V, with a Young's modulus and Poisson's ratio of 114 GPa and 0.34, respectively.[42,56] In agreement with data available in the literature, the Poisson's ratio of bone tissue (both cortical and trabecular) was assumed to be 0.3,[52] Young's modulus of both maxillary and mandibular cortical bone was assumed to be 13.7 GPa,[42,57] and Young's modulus for maxillary (mandibular) cancellous bone was set to 0.5 GPa[52] (1 GPa[42]). These properties approximate type II bone quality,[58] and maxillary trabecular bone was assumed to be less dense than mandibular, resulting in a smaller Young's modulus.[59]

Complete osseous integration between implants and living tissues was assumed, resulting in the continuity of the displacement field at the implant-bone interface. Furthermore, displacement functions were assumed to be continuous at possible interfaces between different implant parts (abutment, internal screw, implant), and the end sections (parallel to the *xz* plane, Fig. 1) of the bone segments were assumed to be fixed; that is, all nodal displacement components of segments were set equal to zero. Since the free length of bone segments (the distance between end surfaces of anatomical sites and the implant location) was sufficiently larger than the maximum dimension of the implant and in agreement with the theory of elasticity, these boundary conditions should not significantly affect the stress results at the periimplant region.

Finite element simulations for the 5 commercial single tooth implants were developed considering a static load applied at the top of abutments without any eccentricity with respect to the implant axis (Fig. 1, *z*), and angled at approximately 22 degrees with reference to *z*. The lateral force component along the buccal-lingual axis (opposed to the *x*-axis direction) was assumed to be 100 N, and the vertical intrusive component was 250 N. To allow for significant comparisons, abutments were adjusted in such a way that all loading application points were 7 mm from the bone insertion surface.

Coupled bone-implant models were numerically analyzed to evaluate stress distributions on both compact and cancellous bone at periimplant regions, providing risk measures of critical bone overloading. In agreement with a number of studies,[33-52] the von Mises stress field (σ_{VM}) was used as an indicator of the average stress level at the periimplant region, providing a global measure of load transfer mechanisms. Moreover, in agreement with the maximum normal stress criterion,[60] principal stresses were used at the bone-implant interface to define local risk indicators of physiological bone failure and of the activation of bone resorption. Accordingly, assuming ultimate bone strength as a physiological limit, local overloading at cortical bone occurs in compression when the maximum compressive principal stress (σ_C) exceeds 170-190 MPa in modulus, and in tension when the maximum tensile principal stress (σ_T) exceeds 100-130 MPa.[17,59] Moreover, local overloading at the trabecular bone occurs when σ_T and/or $|\sigma_C|$ exceed 5 MPa,[17] the symbol $|\sigma_C|$ denoting the modulus of σ_C.

In order to provide quantitative indications that are useful for comparative evaluations, trabecular (Σ_t) and compact (Σ_c) bone layers surrounding the implant and having an average thickness of approximately 1 mm were considered. For a given position along the implant axis, average and peak values of σ_{VM}, σ_T, and σ_C were computed over Σ_c and Σ_t, by using a custom-made postprocessing procedure, with input consisting of some primary geometrical and topological data (nodal coordinates and

TABLE II. Number of elements and nodes used in finite element models of 5 implants

	Maxillary Segment		Mandibular Segment	
Implant	**Elements**	**Nodes**	**Elements**	**Nodes**
ITI Standard (1)	116,677	134,464	102,079	116,052
ITI Standard (2)	108,961	128,282	103,627	122,401
NobelDirect	126,318	146,946	126,318	146,946
Brånemark System	135,838	152,533	147,732	168,328
Ankylos	179,903	210,289	156,793	178,447

elements lying at bone-implant interfacial regions) and stress solutions at finite element integration points.

RESULTS

Figures 3 and 4 show von Mises stress distributions computed for the 5 commercial osseointegrated implants evaluated. With reference to the section view at y=0, stress contours for both maxillary and mandibular bone regions were compared and, to provide significant indications about both compact and trabecular periimplant regions, numerical results are presented as means of the 2 different scales of values.

Figures 5, 6, and 7 summarize peaks and average values of principal and von Mises stress measures at both the mandibular and maxillary periimplant regions. Bar charts in Figure 5 refer to the cortical bone (Σ_c), whereas Figures 6 and 7 show quantitative results computed at the trabecular bone and refer to a subdivision of the periimplant domain Σ_t into 3 different regions along the implant axis: near the crestal interface (Figs. 6

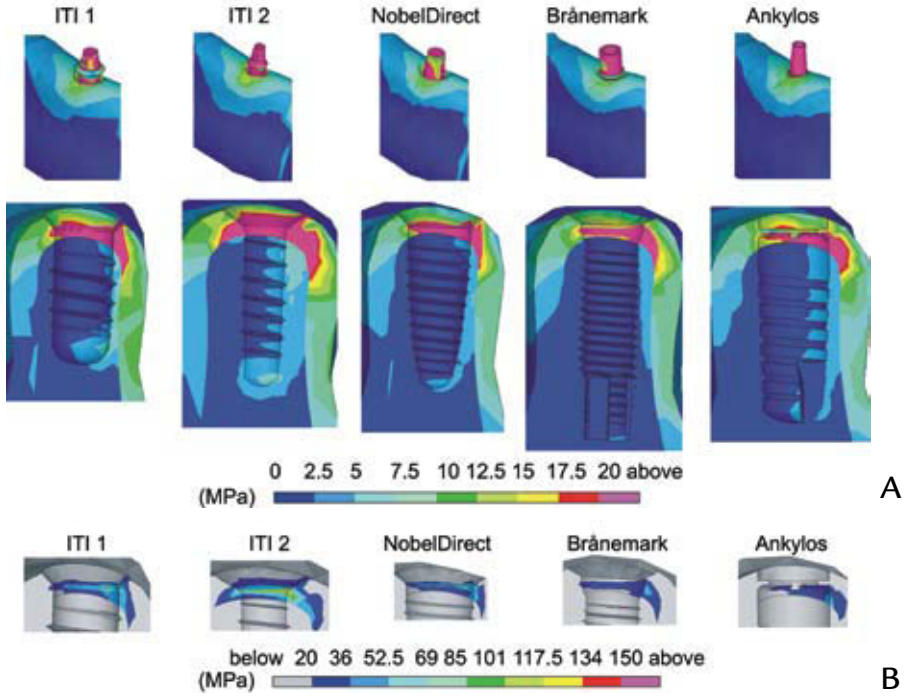

3 A, von Mises stress contours (blue: 0; red: 20 MPa) at section view y=0 for implants in mandibular molar segment. B, Contour details at cortical bone interface (blue: 20; red: 150 MPa).

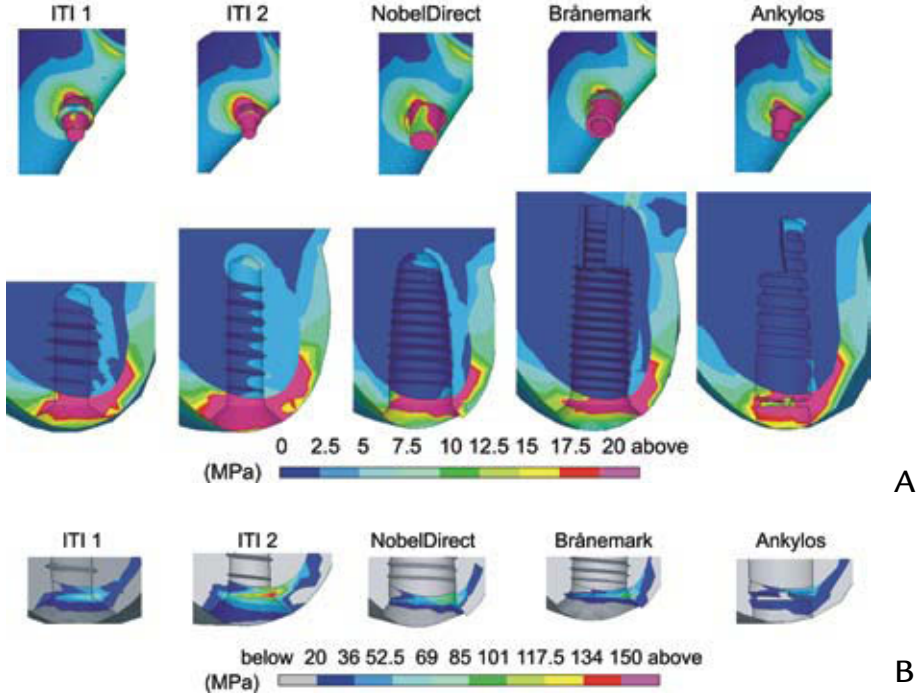

4 A, von Mises stress contours (blue: 0; red: 20 MPa) at section view y=0 for implants in maxillary segment. B, Contour details at cortical bone interface (blue: 20; red: 150 MPa).

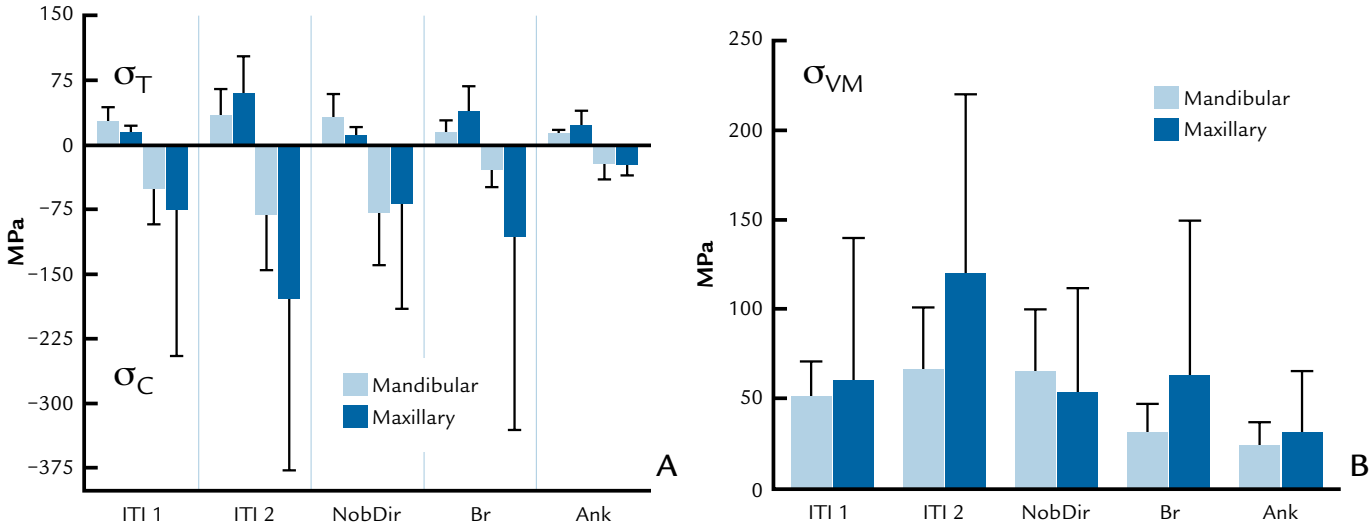

5 von Mises (A, σ_{VM}) and principal (B, σ_C compressive and σ_T tensile) stress measures at cortical bone-implant interface. Average (bars) and peak (lines) values.

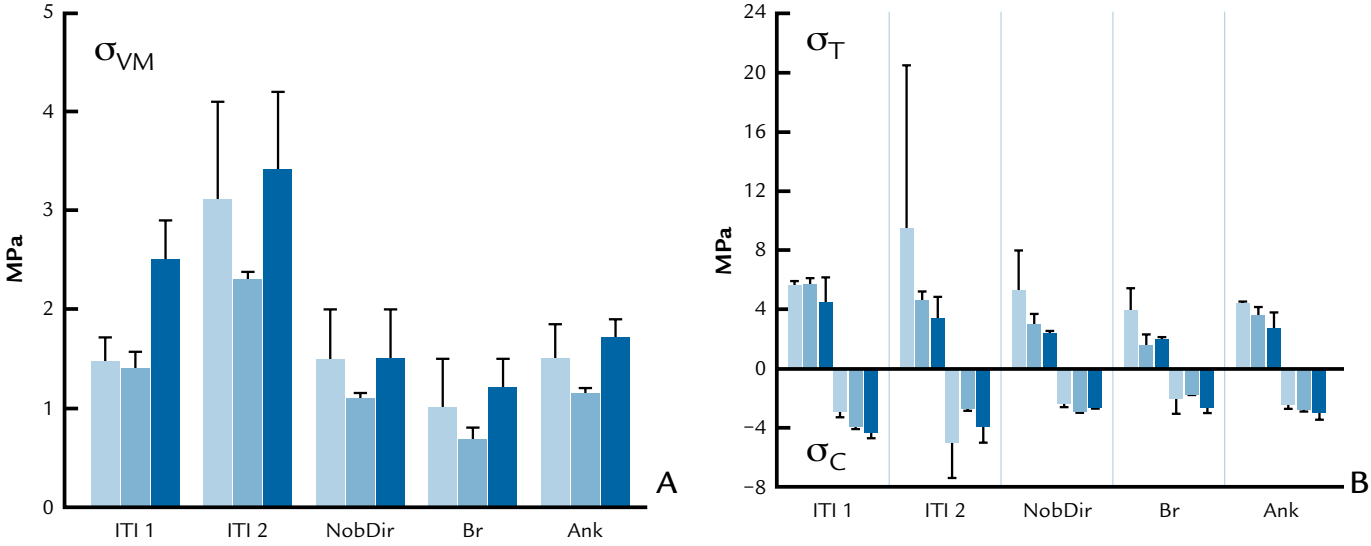

6 von Mises (A, σ_{VM}) and principal (B, σ_C compressive and σ_T tensile) stress measures at trabecular bone-implant interface for mandibular implants. Average (bars) and peak (lines) values computed at 3 different regions along implant axis: near crestal interface (light blue bars), at middle (blue bars), and at lower end (dark blue bars) of implant.

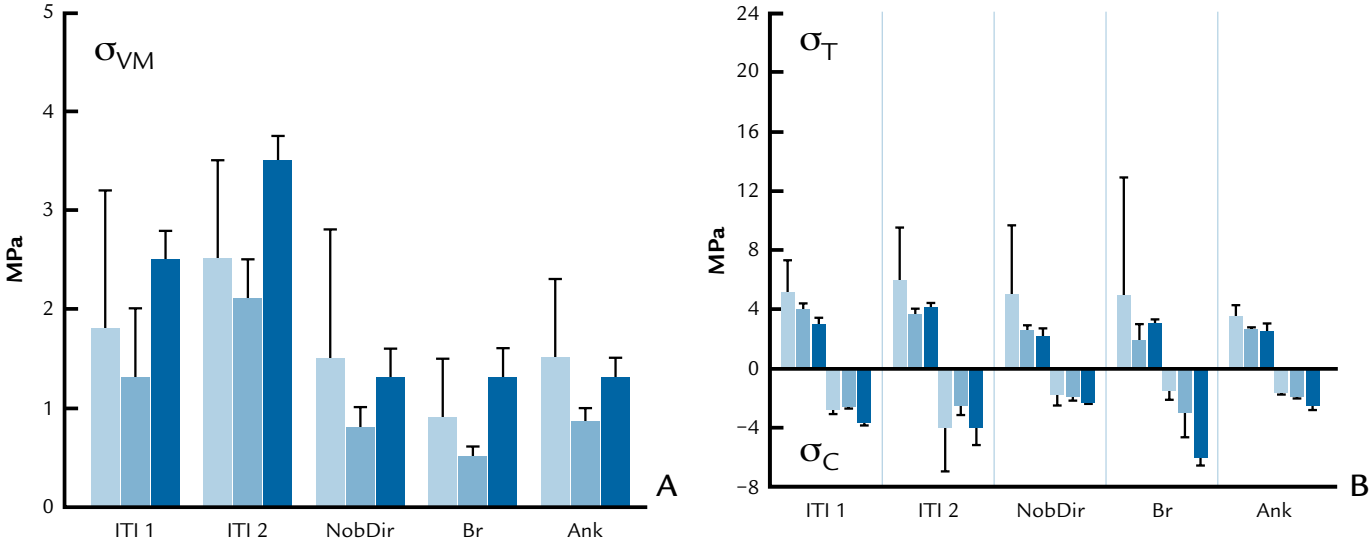

7 von Mises (A, σ_{VM}) and principal (B, σ_C compressive and σ_T tensile) stress measures at trabecular bone-implant interface for maxillary implants. Average (bars) and peak (lines) values computed at 3 different regions along implant axis: near crestal interface (light blue bars), at middle (blue bars), and at lower end (dark blue bars) of implant.

and 7, light blue bars), at the middle (Figs. 6 and 7, blue bars), and at the lower end (Figs. 6 and 7, dark blue bars) of the cancellous bone-implant interface. These 3 parts of Σ_t had the same length along the implant axis.

Stress concentration areas were located at the cortical bone around the implant neck, and the highest values of von Mises and compressive stresses at this region were numerically observed for maxillary implants (σ_{VM} ranging from about 65 MPa (Ankylos) to 220 MPa (ITI Standard 2), compressive stresses $|\sigma_C|$ from about 36 MPa (Ankylos) to approximately 375 MPa (ITI Standard 2)), depending on the implant design and the crestal bone geometry. However, tensile peaks were smaller (σ_T from about 18 MPa to about 100 MPa) than compressive peaks for both the mandibular and maxillary analyses.

The Ankylos implant induced the lowest average and peak values of stress acting on the cortical bone (both in compression and in tension), producing stresses equal to 4 MPa, at the most, at the trabecular bone interface. However, the highest stresses were numerically observed for the NobelDirect and ITI Standard 2 implants on the mandibular segment, and for the ITI Standard 2 implant on the maxillary segment. Average stresses induced by the NobelDirect and ITI Standard 2 implants at the mandibular cortical bone were greater than those of the Ankylos system by approximately 145% in tension and 290% in compression (180% considering σ_{VM}). Furthermore, when the ITI Standard 2 implant was analyzed, stress values in maxillary cortical bone were greater (about 150% in tension, 600% in compression, 300% for the von Mises measure) than for the Ankylos implant. The previously introduced physiological limits in compression, assumed equal to the ultimate bone strength,[17,59] were exceeded at the compact maxillary bone when implants ITI 1, ITI 2, and Brånemark were considered, whereas tensile bone strength limits were never reached.

As far as the overloading risk indicators for cancellous bone were concerned, tensile peaks were always greater than compressive peaks, and significant concentrations appeared at the trabecular-compact interface, as well as, with smaller values, at the lower end of the implant. Strength of cancellous bone (about 5 MPa[17]) was exceeded, primarily in tension, at the concentration areas for all the implants except for Ankylos.

DISCUSSION

The 5 commercial osseointegrated implants that were analyzed by finite element simulations exhibited different stress-based biomechanical behavior, dependent on shape parameters and on the site of placement, as well as on the compact bone geometry at the implant neck. For a given implant, placement in the mandibular and maxillary molar segments induced stress distributions that were dissimilar at the bone-implant interface as a consequence of different geometries and bone mechanical properties, resulting in higher compressive overloading risk in the maxillary segment. For a given implant, the compressive peaks and average stress at the maxillary cortical bone were about 140% of the values for the mandibular one. Accordingly, proposed quantitative stress analysis may help in understanding the clinical evidence that maxillary implants can have a higher incidence of failure than mandibular implants.[7-11]

Simulation results considered functioning implants, modelling crestal bone loss after a healing and loading period. These results have also highlighted the influence of implant length and diameter on load transfer mechanisms. In agreement with the numerically experienced trend proposed by Himmlova et al,[39] Holmgren et al,[41] and Bozkaya et al,[42] maximum implant diameter seems to affect stress peaks at the cortical bone but not at the trabecular region, whereas stress values and distribution at the cancellous bone-implant interface are primarily influenced by implant length. Nevertheless, to control the risk of bone overload and to improve implant biomechanical stress-based performance, numerical results from the current study suggest that implant diameter can be considered to be a more effective design parameter than implant length. In this context, the results of this study can be considered to be complementary to similar, previously published studies.[39,41-44] Due to the simplified and different geometrical models usually used in these studies,[39,41,42] quantitative comparisons cannot be made. Analogously, Carter's[15] hypotheses regarding the influence of the strain level of the bone on hypertrophic responses or bone resorption cannot be directly verified in a quantitative sense, but numerical simulations of the present study have confirmed that the risk of bone overload essentially affects regions around the implant neck.

Stress analysis of implants with similar diameters (such as NobelDirect, ITI 1, and Ankylos) highlights the concept that the risk of overloading compact bone strongly increases when significant crestal bone loss occurs. Accordingly, when crestal bone geometry was modelled by platform switching configurations and subcrestal positioning (as seen with the Ankylos implant), the best stress-based performance for compact bone was obtained, together with acceptable stress values at the cancellous interface. However, when traditional adaptive bone changes were considered (bone conical remodelling after loading), physiological strength limits were exceeded for both the trabecular and compact bone, inducing the risk of further bone loss and jeopardizing implant effectiveness. These results are qualitatively in agreement with those obtained by Maeda et al,[20] although the geometries and loads that were used in that study for the finite element analyses were different from those used in the present study.

In agreement with the numerical

results proposed by Bozkaya et al,[42] present analyses suggest that overloading of the compact bone may occur in compression (due to the lateral components of occlusal load), and that overloading at the interface between cortical and trabecular bone can occur in tension (due to the vertical intrusive loading components). It is worth noting that, in a number of recent numerical studies, the influence of crestal bone loss in functioning implants and of detailed geometrical modelling for the site of placement have been disregarded.[20,39,41-48]

Based on the findings presented here, ossointegrated implants should be chosen and/or designed considering 2 factors: first, that overloading risk at periimplant regions is primarily dependent on implant size (diameter and length) and the site of placement, and secondly, that the biomechanical stress-based performance of implants improves when crestal bone loss is effectively counteracted.

In the current study, even when different crestal bone loss configurations were considered, the ideal condition of 100% osseous integration between implants and bone was assumed. Furthermore, stress analyses were performed assuming a concentrated static load and, as far as the mechanical behavior of bone is concerned, living tissues were modelled as isotropic linearly elastic materials, distinguishing 2 homogeneous material volumes for describing the trabecular and cortical regions. These assumptions do not represent actual clinical conditions because of possible osseointegration defects at the periimplant region and time-dependent, functionally distributed forces, as well as anisotropic, nonhomogeneous, and nonlinear responses of bone. Nevertheless, in that bone modelling and remodelling were beyond the scope of this investigation, and in agreement with a number of well-established numerical results,[20,31-52] the present assumptions can be considered acceptable in a computational sense, to deduce significant and clinically useful indications. In future studies, modelling the bone as an anisotropic and nonhomogeneous regenerative tissue that responds to stress by resorption or regeneration under load would be an improvement in current finite element models to address the issues found in this study.

CONCLUSIONS

Within the limitations of this study, numerical simulations showed that implant design (in terms of both implant diameter and length), crestal bone geometry, and placement site affect the mechanisms of load transmission. Cortical periimplant areas that could be affected by overloading were influenced primarily by implant diameter, irrespective of bone-implant interface length. However, an increase in implant length reduced stress gradients at the cancellous periimplant region. Crestal bone geometries characterized by low levels of bone loss and clinically associated with platform switching configurations exhibited effective stress-based performance, resulting in a reduction in the risk of overloading at the implant neck with respect to induced cratering of bone. Possible risk of tissue overloading occurred in compression for the compact bone (due to the lateral components of the occlusal load) and in tension at the interface between the cortical and trabecular bone (due to the vertical intrusive loading components). Furthermore, higher risk was numerically demonstrated for placement of maxillary implants than for mandibular ones.

REFERENCES

1. Weyant R. Short-term clinical success of root-form titanium implant systems. J Evid Based Dent Pract 2003;3:127-30.
2. Roos-Jansåker AM, Lindahl C, Renvert H, Renvert S. Nine- to fourteen-year follow-up of implant treatment. Part I: implant loss and associations to various factors. J Clin Periodontol 2006;33:283-9.
3. Tonetti MS. Determination of the success and failure of root-form osseointegrated dental implants. Adv Dent Res 1999;13:173-80.
4. Romeo E, Chiapasco M, Ghisolfi M, Vogel G. Long-term clinical effectiveness of oral implants in the treatment of partial edentulism. Seven-year life table analysis of a prospective study with ITI dental implants system used for single-tooth restorations. Clin Oral Implants Res 2002;13:133-43.
5. Adell R, Lekholm U, Rockler B, Brånemark PI. A 15-year study of osseointegrated implants in the treatment of the endentulous jaw. Int J Oral Surg 1981;10:387-416.
6. Ericsson I, Nilson H, Lindh T, Nilner K, Randow K. Immediate functional loading of Brånemark single tooth implants. An 18 months' clinical pilot follow-up study. Clin Oral Implants Res 2000;11:26-33.
7. Piattelli A, Scarano A, Piattelli M. Microscopical aspects of failure in osseointegrated dental implants: a report of five cases. Biomaterials 1996;17:1235-41.
8. Jemt T, Chai J, Harnett J, Heath MR, Hutton JE, Johns RB, et al. A 5-year prospective multicenter follow-up report on overdentures supported by osseointegrated implants. Int J Oral Maxillofac Implants 1996;11:291-8.
9. Eckert SE, Wollan PC. Retrospective review of 1170 endosseous implants placed in partially edentulous jaws. J Prosthet Dent 1998;79:415-21.
10. Lekholm U, Gunne J, Henry P, Higuchi K, Linden U, Bergstrom C, et al. Survival of the Brånemark implant in partially edentulous jaws: a 10-year prospective multicenter study. Int J Oral Maxillofac Implants 1999;14:639-45.
11. Drago CJ. Rates of osseointegration of dental implants with regard to anatomical location. J Prosthodont 1992;1:29-31.
12. Watzek G. Endosseous implants: scientific and clinical aspects. Chicago: Quintessence; 1996. p. 291-317.
13. Brunski JB. Biomechanics of dental implants. In: Block MS, Kent JN, Guerra LR, editors. Implants in dentistry: essentials of endosseous implants for maxillofacial reconstruction. Philadelphia: W.B. Saunders; 1997. p. 63-71.
14. Irving JT. Factors concerning bone loss associated with periodontal disease. J Dent Res 1970;49:262-7.
15. Carter DR, Van Der Meulen MC, Beaupré GS. Mechanical factors in bone growth and development. Bone 1996;18(1 Suppl):5S-10S.
16. Cowin SC. Bone mechanics handbook. 2nd ed. Boca Raton: CRC Press; 2001. p. I 1-55.
17. Martin RB, Burr DB, Sharkey NA. Skeletal tissue mechanics. New York: Springer; 1998. p. 127-78.
18. Gardner DM. Platform switching as a means to achieving implant esthetics. N Y State Dent J 2005;71:34-7.
19. Lazzara RJ, Porter SS. Platform switching: a new concept in implant dentistry for controlling postrestorative crestal bone levels. Int J Periodontics Restorative Dent 2006;26:9-17.
20. Maeda Y, Miura J, Taki I, Sogo M. Biomechanical analysis on platform switching: is there any biomechanical rationale? Clin Oral Implants Res 2007;18:581-4.

21. Berglundh T, Lindhe J. Dimension of the periimplant mucosa. Biological width revisited. J Clin Periodontol 1996;23:971-3.
22. Cochran DL, Hermann JS, Schenk RK, Higginbottom FL, Buser D. Biologic width around titanium implants. A histometric analysis of the implanto-gingival junction around unloaded and loaded nonsubmerged implants in the canine mandible. J Periodontol 1997;68:186-98.
23. Kan JY, Rungcharassaeng K, Umezu K, Kois JC. Dimensions of peri-implant mucosa: an evaluation of maxillary anterior single implants in humans. J Periodontol 2003;74:557-62.
24. Hermann JS, Cochran DL, Nummikoski PV, Buser D. Crestal bone changes around titanium implants. A radiographic evaluation of unloaded nonsubmerged and submerged implants in the canine mandible. J Periodontol 1997;68:1117-30.
25. Oakley E, Rhyu IC, Karatzas S, Gandini-Santiago L, Nevins M, Caton J. Formation of the biologic width following crown lengthening in nonhuman primates. Int J Periodontics Restorative Dent 1999;19:529-41.
26. Hermann JS, Schoolfield JD, Schenk RK, Buser D, Cochran DL. Influence of the size of the microgap on crestal bone changes around titanium implants. A histometric evaluation of unloaded non-submerged implants in the canine mandible. J Periodontol 2001;72:1372-83.
27. Hermann F, Lerner H, Palti A. Factors influencing the preservation of the periimplant marginal bone. Implant Dent 2007;16:165-75.
28. Misch CE, Bidez MW. A scientific rationale for dental implant design. In: Misch CE, editor. Contemporary implant dentistry. 3rd ed. St. Louis: Mosby; 2007. p. 329-44.
29. Cochran DL. A comparison of endosseous dental implant surfaces. J Periodontol 1999;70:1523-39.
30. Fernàndez E, Gil FJ, Aparicio C, Nilsson M, Sarda S, Rodriguez D, et al. Materials in dental implantology. In: Natali AN, editor. Dental biomechanics. London: Taylor & Francis; 2003. p. 69-89.
31. Natali AN, Pavan PG. Numerical approach to dental biomechanics. In: Natali AN, editor. Dental biomechanics. London: Taylor & Francis; 2003. p. 211-39.
32. Natali AN, Pavan PG. A comparative analysis based on different strength criteria for evaluation of risk factor for dental implants. Comput Methods Biomech Biomed Engin 2002;5:127-33.
33. Geng IP, Tan KB, Liu GR. Application of finite element analysis in implant dentistry: a review of the literature. J Prosthet Dent 2001;85:585-98.
34. Van Staden RC, Guan H, Loo YC. Application of the finite element method in dental implant research. Comput Methods Biomech Biomed Engin 2006;9:257-70.
35. Siegele D, Soltesz U. Numerical investigations of the influence of implant shape on stress distribution in the jaw bone. Int J Oral Maxillofac Implants 1989;4:333-40.
36. Rieger MR, Adams WK, Kinzel GL. A finite element survey of eleven endosseous implants. J Prosthet Dent 1990;63:457-65.
37. Chun HJ, Cheong SY, Han JH, Heo SJ, Chung JP, Rhyu IC, et al. Evaluation of design parameters of osseointegrated dental implants using finite element analysis. J Oral Rehabil 2002;29:565-74.
38. Petrie CS, Williams JL. Comparative evaluation of implant designs: influence of diameter, length, and taper on strains in the alveolar crest. A three-dimensional finite-element analysis. Clin Oral Implants Res 2005;16:486-94.
39. Himmlová L, Dostálová T, Kácovsky A, Konvicková S. Influence of implant length and diameter on stress distribution: a finite element analysis. J Prosthet Dent 2004;91:20-5.
40. Akpinar I, Demirel F, Parnas L, Sahin S. A comparison of stress and strain distribution characteristics of two different rigid implant designs for distal-extension fixed prostheses. Quintessence Int 1996;27:11-7.
41. Holmgren EP, Seckinger RJ, Kilgren LM, Mante F. Evaluating parameters of osseointegrated dental implants using finite element analysis-- a two dimensional comparative study examining the effects of implant diameter, implant shape, and load direction. J Oral Implantol 1998;24:80-8.
42. Bozkaya D, Muftu S, Muftu A. Evaluation of load transfer characteristics of five different implants in compact bone at different load levels by finite elements analysis. J Prosthet Dent 2004;92:523-30.
43. Chun HJ, Shin HS, Han CH, Lee SH. Influence of implant abutment type on stress distribution in bone under various loading conditions using finite element analysis. Int J Oral Maxillofac Implants 2006;21:195-202.
44. Meijer HJ, Starmans FJ, Steen WH, Bosman F. Loading conditions of endosseous implants in an edentulous human mandible: a three-dimensional, finite-element study. J Oral Rehabil 1996;23:757-63.
45. Alkan I, Sertgöz A, Ekici B. Influence of occlusal forces on stress distribution in preloaded dental implant screws. J Prosthet Dent 2004;91:319-25.
46. Kitagawa T, Tanimoto Y, Nemoto K, Aida M. Influence of cortical bone quality on stress distribution in bone around dental implant. Dent Mater J 2005;24:219-24.
47. Lin CL, Kuo YC, Lin TS. Effects of dental implant length and bone quality on biomechanical responses in bone around implants: a 3-D non-linear finite element analysis. Biomed Eng Appl Basis Comm 2005;17:44-9.
48. Saab XE, Griggs JA, Powers JM, Engelmeier RL. Effect of abutment angulation on the strain on the bone around an implant in the anterior maxilla: a finite element study. J Prosthet Dent 2007;97:85-92.
49. Yokoyama S, Wakabayashi N, Shiota M, Ohyama T. The influence of implant location and length on stress distribution for three-unit implant-supported posterior cantilever fixed partial dentures. J Prosthet Dent 2004;91:234-40.
50. Natali AN, Pavan PG, Ruggero AL. Evaluation of stress induced in peri-implant bone tissue by misfit in multi-implant prosthesis. Dent Mater 2006;22:388-95.
51. Chen F, Terada K, Hanada K, Saito I. Anchorage effects of a palatal osseointegrated implant with different fixation: a finite element study. Angle Orthod 2005;75:593-601.
52. Chun HJ, Park DN, Han CH, Heo SJ, Heo MS, Koak JY. Stress distributions in maxillary bone surrounding overdenture implants with different overdenture attachments. J Oral Rehabil 2005;32:193-205.
53. Callan DP, O'Mahony A, Cobb CM. Loss of crestal bone around dental implants: a retrospective study. Implant Dent 1998;7:258-66.
54. Shin YK, Han CH, Heo SJ, Kim S, Chun HJ. Radiographic evaluation of marginal bone level around implants with different neck designs after 1 year. Int J Oral Maxillofac Implants 2006;21:789-94.
55. Zienkiewicz OC, Taylor RL. The finite element method. Vol. 1, 6th ed. Oxford: Butterworth-Heinemann; 2005. p. 164-99.
56. Lemon JE, Dietsh-Misch F. Biomaterials for dental implants. In: Misch CE, editor. Contemporary implant dentistry. 3rd ed. St. Louis: Mosby; 2007. p. 271-302.
57. Van Oosterwyck H, Duyck J, Vander Sloten J, Van der Perre G, De Cooman M, Lievens S, et al. The influence of bone mechanical properties and implant fixation upon bone loading around oral implants. Clin Oral Implants Res 1998;9:407-18.
58. Lekholm U, Zarb GA. Patient selection and preparation. In: Brånemark PI, Zarb GA, Albrektsson T, editors. Tissue-integrated prostheses: osseointegration in clinical dentistry. Chicago: Quintessence; 1985. p. 199-209.
59. Natali AN, Hart RT, Pavan PG, Knets I. Mechanics of bone tissue. In: Natali AN, editor. Dental biomechanics. London: Taylor & Francis; 2003. p. 1-19.
60. Mendelson A. Plasticity: theory and application. New York: Collier-MacMillan; 1968. p. 71-2.

Corresponding author:
Dr Luigi Baggi
Dipartimento di Scienze Odontostomatologiche
Università di Roma "Tor Vergata"
Viale Oxford 81
00133 Rome
ITALY
Fax: 0039-0672597005
E-mail: luigi.baggi@uniroma2.it or vairo@ing.uniroma2.it

Acknowledgements
This work was developed within the framework of the Lagrange Laboratory, a European research group involving CNRS (Centre National de la Recherche Scientifique, France), CNR (Consiglio Nazionale delle Ricerche, Italy), Universities of Rome "Tor Vergata," Calabria, Cassino, Pavia, Salerno, Ecole Polytechnique, University of Montpellier II, ENPC (École Nationale des Ponts et Chaussées, France), LCPC (Laboratoire Central des Ponts et Chaussées, France), and ENTPE (École Nationale des Travaux Publics de l'État, France).